Electronic Supplementary Material (ESI) for Physical Chemistry Chemical Physics.

A Force Field for Bio-Polymers in Ionic Liquids (BILFF) – Part 1: [EMIm][OAc] / Water Mixtures

Supporting Information

Eliane Roos and Martin Brehm*

Institut für Chemie - Theoretische Chemie, Martin-Luther-Universität Halle-Wittenberg,
Von-Danckelmann-Platz 4, 06120 Halle (Saale), Germany.

*E-mail: Martin_Brehm@gmx.de

*Website: https://brehm-research.de/

Force Field Parameters

In this section, we report our optimized force field parameters for the 1-ethyl-3-methylimidazolium cation and the acetate anion. The parameters are compatible to OPLS–AA.[1–3] In accordance to OPLS–AA, the non-bonded Lennard-Jones and Coulomb interactions for 1–2 and 1–3 neighbors are neglected, while those for 1–4 neighbors are scaled with a factor of 0.5 (see scaling factor f_{ij} in Equation 1 below). Geometric mixing rules are applied for the Lennard-Jones interactions. We used a Coulomb and Lennard-Jones cutoff radius of 800 pm and a PPPM long-range Coulomb solver *(as implemented in LAMMPS)*[4] in all our simulations.

When simulating mixtures with water, the TIP4P–EW force field[5] *(with fixed bonds and angles)* has been applied for the water molecules. These parameters have not been modified within this work, they are used as reported in the original publication.

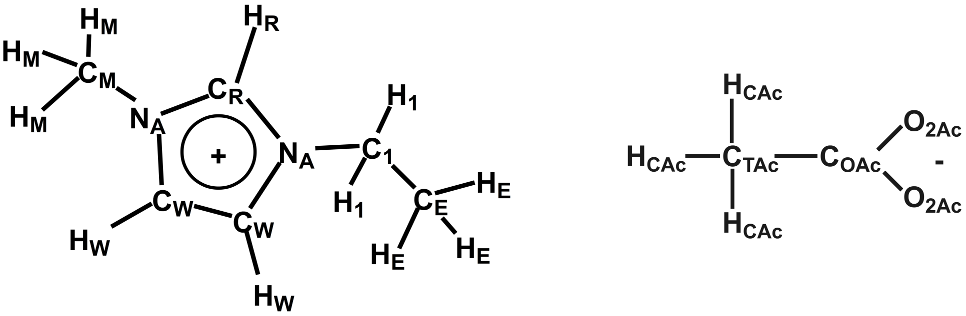

Figure S-1: Atom types in the 1-ethyl-3-methylimidazolium cation *(left)* and the acetate anion *(right)*. For the corresponding atom classes, see Table S-1.

Table S-1: Atom types *(see Figure S-1)* and corresponding atom classes for the 1-ethyl-3-methylimidazolium cation *(upper part)* and the acetate anion *(lower part)*. The atom types are used for the non-bonded interactions *(see Table S-2)*, while the atom classes are used for the bonded interactions *(see Tables S-3 to S-6)*.

Atom Type	Atom Class
CR	CR
C1	CT
CE	CT
CM	CT
CW	CW
HR	HA
HW	HA
H1	HC
HE	HC
HM	HC
NA	NA
COAc	CO
CTAc	CT
HCAc	HC
O2Ac	O2

The potential energy in OPLS–AA is calculated according to the following equation:

$$
\begin{aligned}
U(r^N) = &\sum_{\text{bonds}}^{i} \frac{k_l}{2}(l_i - l_{i,0})^2 + \sum_{\text{angles}}^{i} \frac{k_\theta}{2}(\theta_i - \theta_{i,0})^2 \\
&+ \sum_{\text{dihedrals}}^{i} [\frac{V_1^i}{2}[1 + cos(\phi_\mathrm{i})] + \frac{V_2^i}{2}[1 - cos(2\phi_\mathrm{i})] + \frac{V_3^i}{2}[1 + cos(3\phi_\mathrm{i})]] \qquad (1) \\
&+ \sum_{i=1}^{N} \sum_{j=i+1}^{N} \left[4\epsilon_{ij} \left[\left(\frac{\sigma_{ij}}{r_{ij}}\right)^{12} - \left(\frac{\sigma_{ij}}{r_{ij}}\right)^{6} \right] + \frac{q_i q_j e^2}{4\pi\epsilon_0 r_{ij}} \right] f_{ij} \,.
\end{aligned}
$$

Table S-2: Atomic partial charges q (total ion charge ±0.82) and Lennard-Jones parameters σ and ϵ for the 1-ethyl-3-methylimidazolium cation *(upper part)* and the acetate anion *(lower part)*. For the atom types, see Figure S-1.

Atom Type	q	σ / Å	ϵ / kJ mol^{-1}
C1	−0.147	3.34	0.276
CE	−0.042	3.34	0.276
CM	−0.147	3.34	0.276
CR	−0.096	3.38	0.293
CW	−0.113	3.38	0.293
H1	+0.116	2.38	0.126
HE	+0.055	2.38	0.126
HM	+0.116	2.38	0.126
HR	+0.165	1.43	0.126
HW	+0.150	1.62	0.126
NA	+0.134	3.10	0.711
COAc	+0.575	3.57	0.439
CTAc	−0.230	3.34	0.276
HCAc	+0.049	2.38	0.126
O2Ac	−0.656	2.96	0.879

Please note: The force constants k for the bonds and angles and the torsion parameters V do **not** include the factor $\frac{1}{2}$ from the potential energy equation *(see Equation 1)*.

Table S-3: Bond equilibrium lengths l_0 and force constants k_l for the 1-ethyl-3-methylimidazolium cation and the acetate anion. For the atom classes, see Table S-1.

Bond Type	l_0 / Å	k_l / kJ mol^{-1} Å^{-2}
CO–O2	1.284	4457
CR–HA	1.089	2570
CT–CO	1.554	1820
CT–CT	1.532	2097
CT–HC	1.099	3013
CW–CW	1.374	4019
CW–HA	1.085	2943
NA–CR	1.356	3636
NA–CT	1.485	2078
NA–CW	1.403	2775

Table S-4: Angle equilibrium values θ_0 and force constants k_θ for the 1-ethyl-3-methylimidazolium cation and the acetate anion. For the atom classes, see Table S-1.

Angle Type	θ_0 / Deg	k_θ / kJ mol^{-1} rad^{-2}
O2–CO–O2	127.2	790.6
CT–CO–O2	117.7	524.4
NA–CR–HA	126.2	244.9
NA–CR–NA	107.6	831.0
CO–CT–HC	110.3	303.6
CT–CT–HC	111.4	338.6
HC–CT–HC	109.2	308.0
NA–CT–CT	110.9	532.7
NA–CT–HC	107.2	411.7
CW–CW–HA	131.7	236.7
NA–CW–CW	107.0	805.7
NA–CW–HA	120.8	263.0
CR–NA–CW	110.0	842.8
CT–NA–CR	124.9	370.2
CT–NA–CW	125.2	367.8

Table S-5: Torsion parameters V_n for the 1-ethyl-3-methylimidazolium cation and the acetate anion. For the atom classes, see Table S-1.

Torsion Angle Type	V_1 / $\mathrm{kJ\,mol^{-1}}$	V_2 / $\mathrm{kJ\,mol^{-1}}$	V_3 / $\mathrm{kJ\,mol^{-1}}$
CT–NA–CR–NA	0.000	19.460	0.000
CT–NA–CR–HA	0.000	19.460	0.000
CW–NA–CR–NA	0.000	39.000	0.000
CW–NA–CR–HA	0.000	19.460	0.000
CR–NA–CT–HC	0.000	0.000	0.000
CR–NA–CT–CT	10.540	0.000	0.000
CW–NA–CT–HC	0.000	0.000	0.519
CW–NA–CT–CT	14.300	−12.200	−1.590
CR–NA–CW–HA	0.000	12.550	0.000
CR–NA–CW–CW	0.000	25.000	0.000
CT–NA–CW–HA	0.000	12.550	0.000
CT–NA–CW–CW	0.000	12.550	0.000
HC–CT–CT–HC	0.000	0.000	1.255
NA–CT–CT–HC	0.000	0.000	0.367
HC–CT–CO–O2	0.000	0.000	0.000
HA–CW–CW–HA	0.000	30.000	0.000
NA–CW–CW–HA	0.000	44.980	0.000
NA–CW–CW–NA	0.000	65.000	0.000

Please note: Improper torsions are handled as torsions; there is no extra term for impropers in the potential energy equation.

Table S-6: Improper torsions for the 1-ethyl-3-methylimidazolium cation and the acetate anion. For the atom classes, see Table S-1.

Improper Torsion Type	V_1 / $\mathrm{kJ\,mol^{-1}}$	V_2 / $\mathrm{kJ\,mol^{-1}}$	V_3 / $\mathrm{kJ\,mol^{-1}}$
NA–CW–CW–HA	0.000	8.200	0.000
CR–CW–NA–CT	0.000	8.370	0.000
CR–CW–NA–HA	0.000	8.370	0.000
NA–NA–CR–CT	0.000	9.200	0.000
NA–NA–CR–HA	0.000	9.900	0.000
CT–O2–CO–O2	0.000	90.000	0.000

Radial Distribution Functions

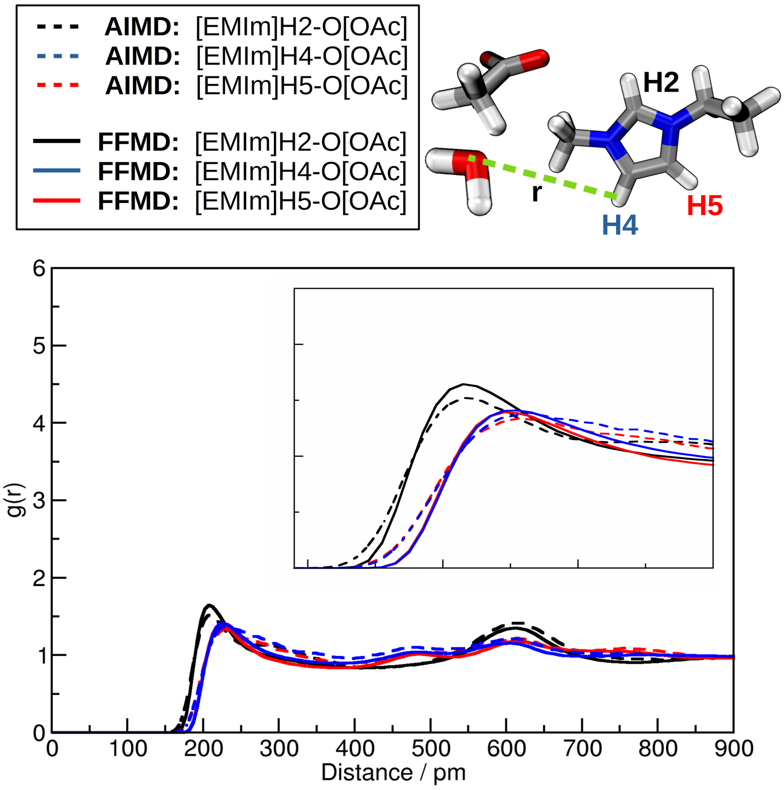

Figure S-2: Comparison of the radial distribution functions (RDFs) of the AIMD and the force field MD using BILFF between the hydrogen atoms H2, H4 and H5 of $[EMIm]^+$ and the oxygen atom of water in the aqueous ionic liquid.

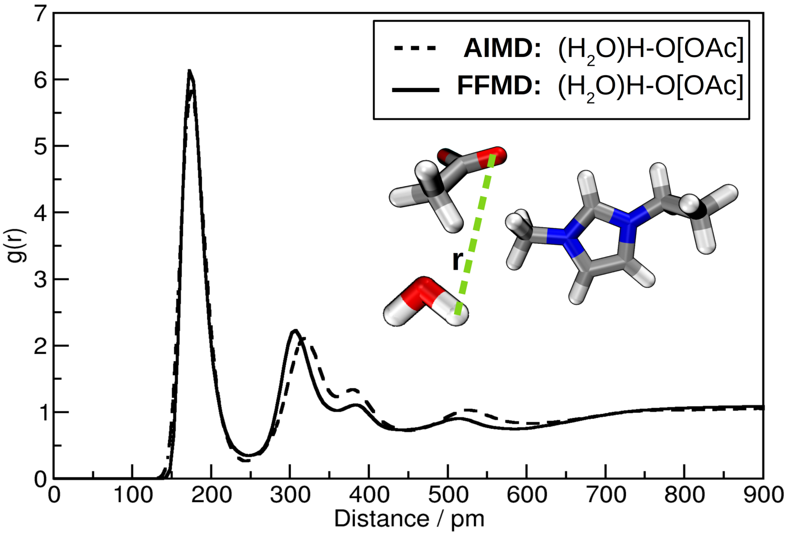

Figure S-3: Comparison of the radial distribution functions (RDFs) of the AIMD and the force field MD using BILFF between the hydrogen atoms of water and the oxygen atoms of acetate in the aqueous ionic liquid.

Combined Distribution Functions

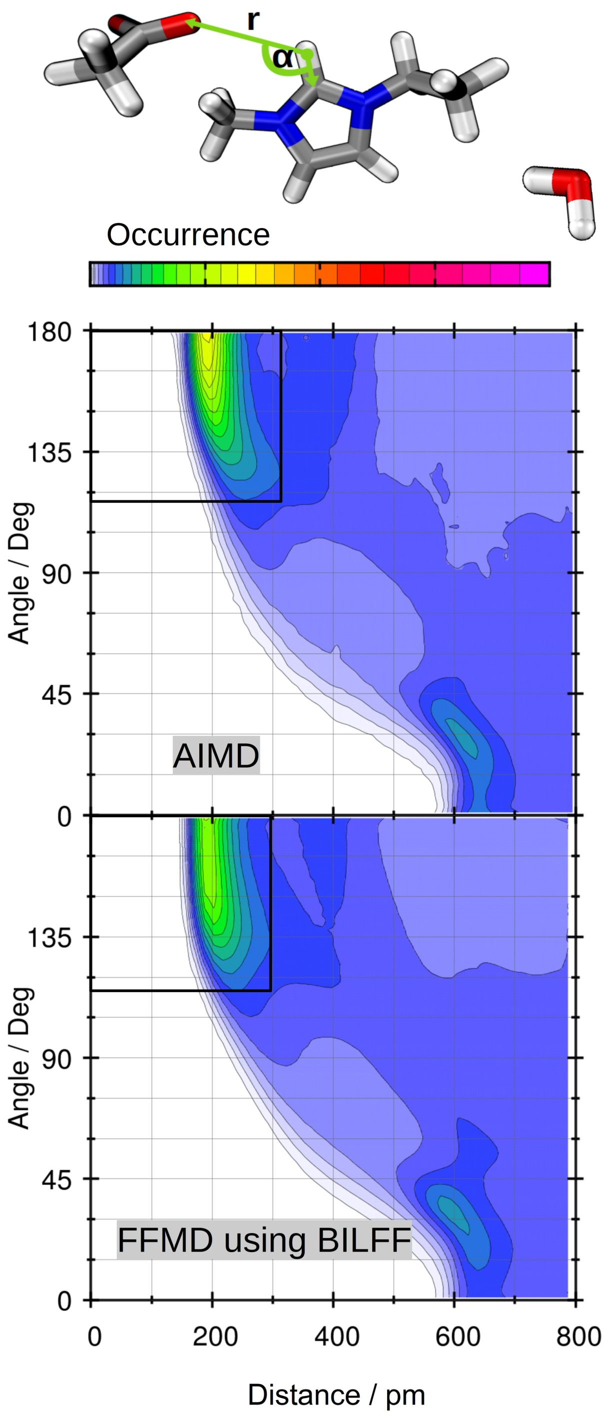

Figure S-4: Combined distribution functions (CDFs) from the AIMD *(upper panel)* and the force-field MD using BILFF *(lower panel)* between the hydrogen atom H2 of $[\text{EMIm}]^+$ and the acetate oxygen in the aqueous ionic liquid with marked geometric criterion for the dimer autocorrelation function of this hydrogen bond *(black rectangle)*.

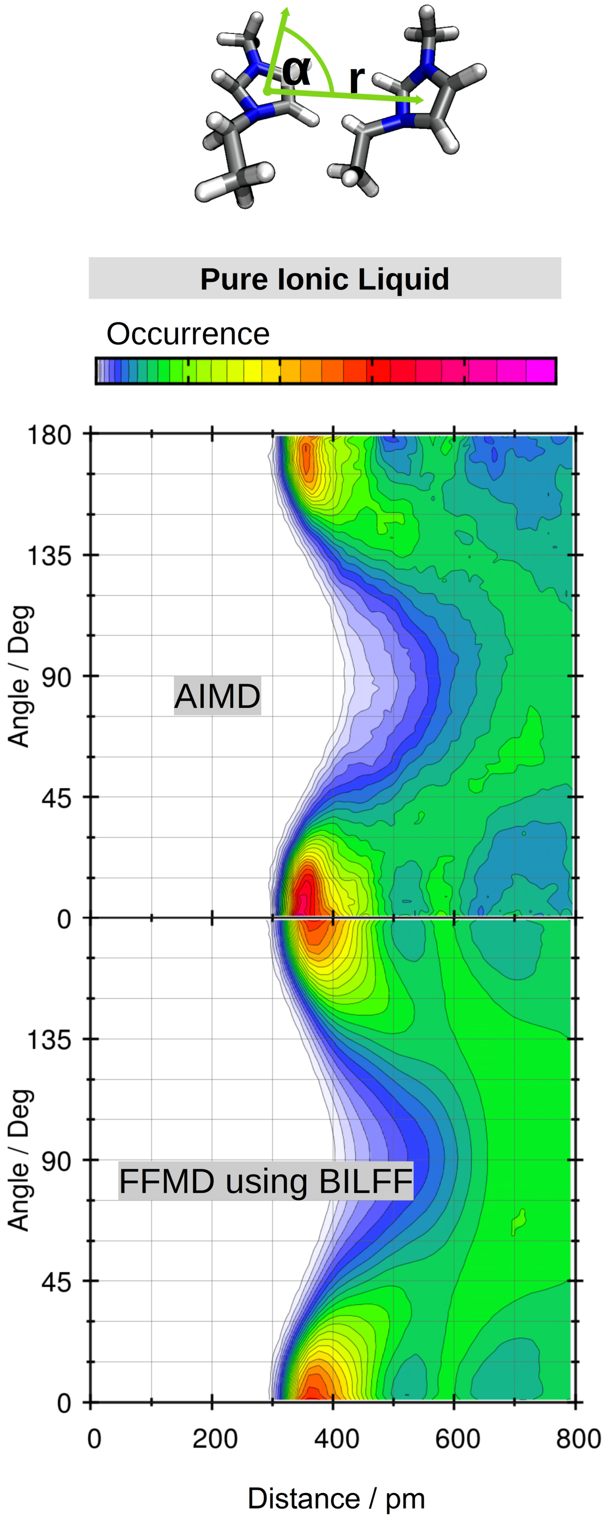

Figure S-5: Combined distribution functions (CDFs) from the AIMD *(upper panel)* and the force field MD using BILFF *(lower panel)* between the ring centers of two [EMIm]$^+$ cations in the pure ionic liquid.

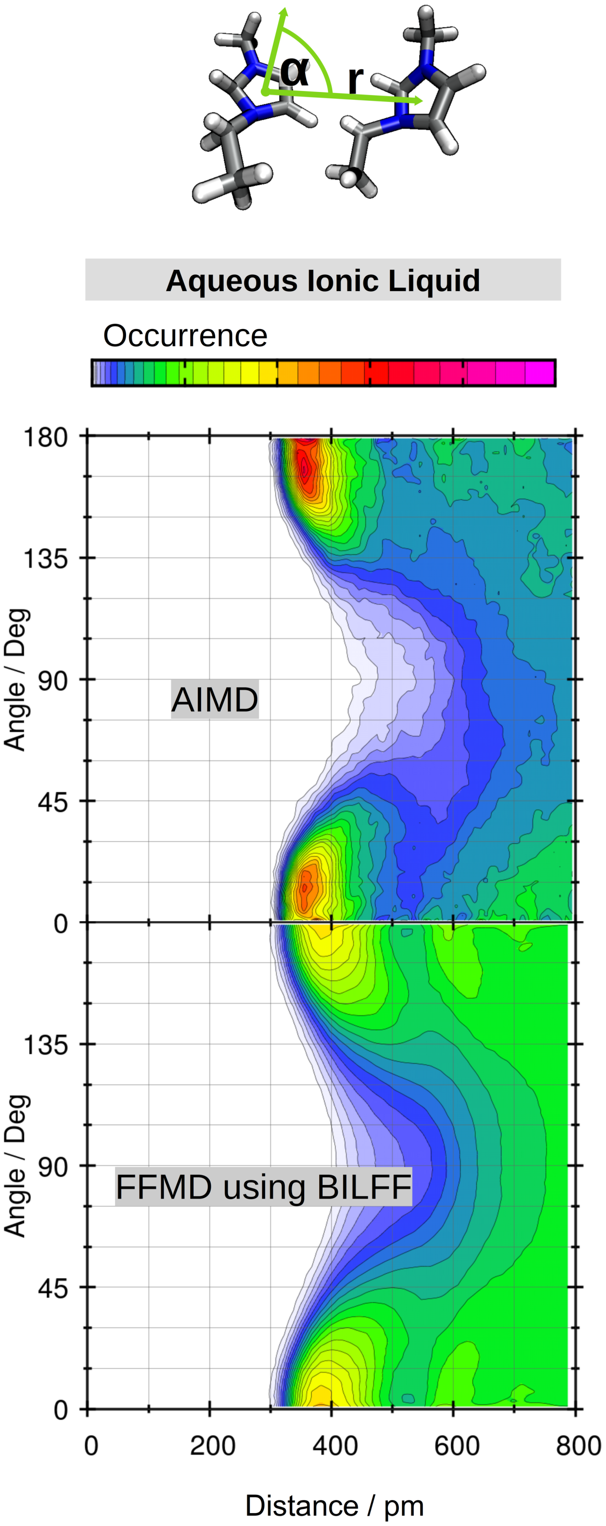

Figure S-6: Combined distribution functions (CDFs) from the AIMD *(upper panel)* and the force field MD using BILFF *(lower panel)* between the ring centers of two $[EMIm]^+$ cations in the aqueous ionic liquid.

Arrhenius Plot of the Diffusion Coefficients

Figures S-7 and Fig. S-8 show the Arrhenius plots of the calculated diffusion coefficients at different temperatures of pure and aqueous [EMIm][OAc]. The linear shape in the logarithmic–reciprocal plots indicates an Arrhenius behavior of the diffusion coefficients, which is frequently observed for ionic liquids.[6]

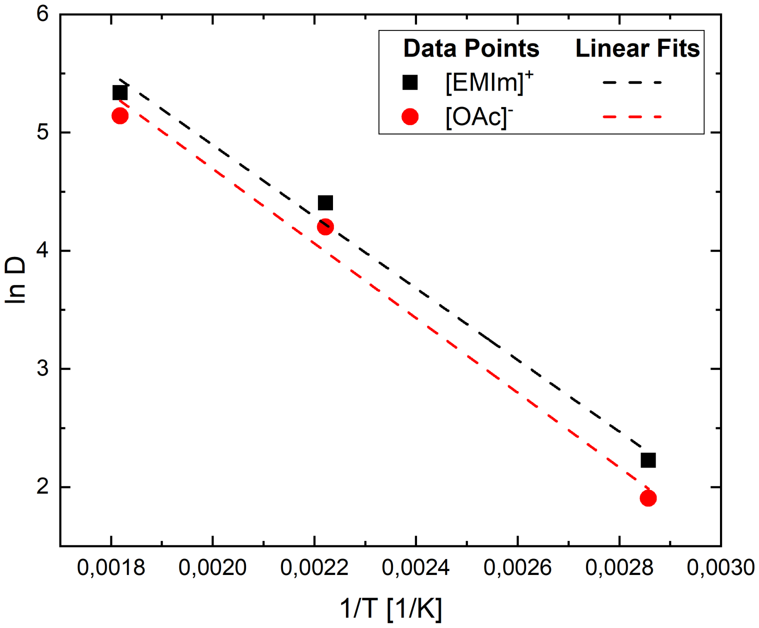

Figure S-7: Arrhenius plot of the calculated diffusion coefficients from our FFMD simulations of the pure system using BILFF.

Table S-7: Regression parameters of the linear regression $y = m \cdot x + n$ in the corresponding Arrhenius plots, Fig. S-7 and S-8.

System	Parameter	[EMIm]$^+$	[OAc]$^-$	H_2O
pure	n	10.96 ± 0.71	11.01 ± 0.82	–
	m	-3032 ± 304	-3159 ± 350	–
	R^2	0.980	0.976	–
aqueous	n	11.47 ± 0.59	11.50 ± 0.22	12.40 ± 0,15
	m	-2917 ± 252	-2928 ± 95	-2926 ± 64
	R^2	0.985	0.998	0.999

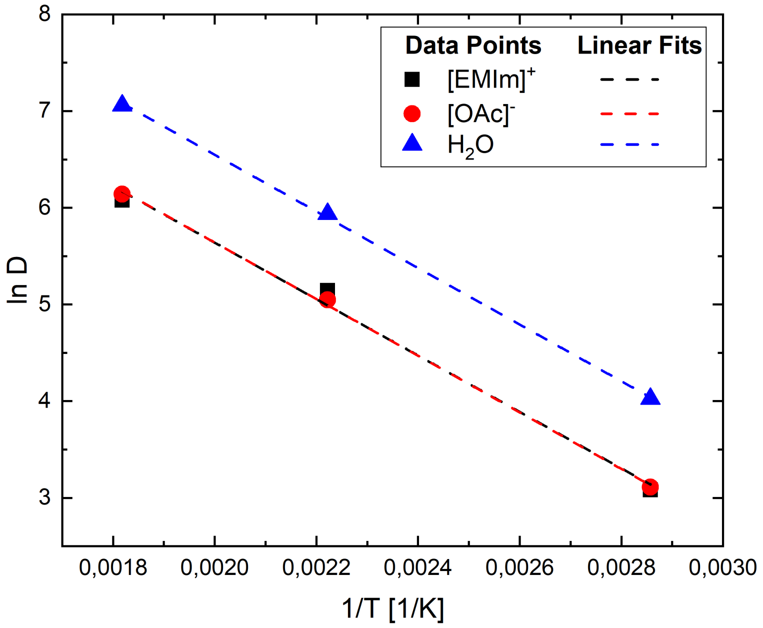

Figure S-8: Arrhenius plot of the calculated diffusion coefficients from our FFMD simulations of the aqueous system using BILFF.

Diffusive Regime

The double logarithmic plot of the mean squared displacement (MSD) over the correlation depth (see Fig. S-9) shows whether the dynamics of a system is diffusive or subdiffusive.[7,8] For both the pure and the aqueous system, a convergence towards a slope of 1 with increasing correlation depth is recognizable. At a temperature of 350 K, a slope of 1 (and thus a diffusive dynamics) is only reached at large correlation depths of around 1 ns in the pure IL.

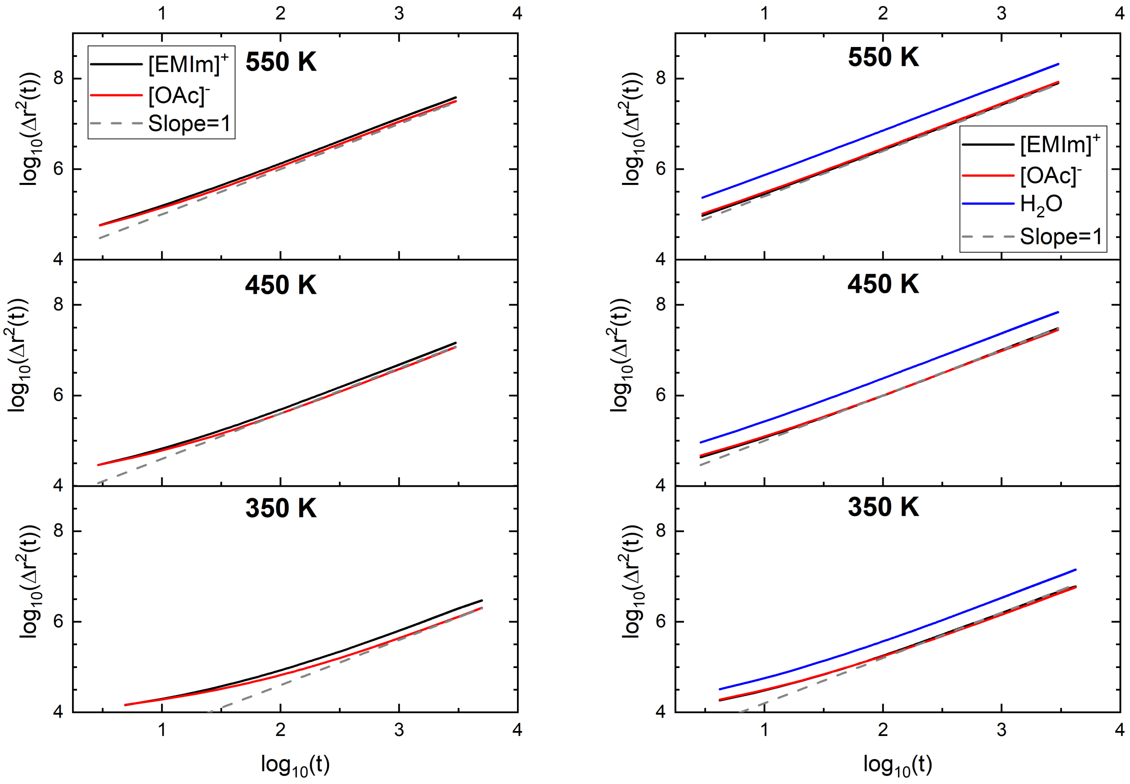

Figure S-9: The double logarithmic plot of the mean squared displacement (MSD) over the correlation depth of the pure (*left*) and aqueous (*right*) system at different temperatures. The dashed lines indicate a slope of 1, *i. e.*, diffusive behavior.

References

(1) Jorgensen, W. L.; Maxwell, D. S.; Tirado-Rives, J. Development and Testing of the OPLS All-Atom Force Field on Conformational Energetics and Properties of Organic Liquids. *J. Am. Chem. Soc.* **1996**, *118*, 11225–11236.

(2) Ponder, J. W.; Case, D. A. *Protein Simulations*; Advances in Protein Chemistry; Elsevier, 2003; Vol. 66; pp 27–85.

(3) Sambasivarao, S. V.; Acevedo, O. Development of OPLS-AA Force Field Parameters for 68 Unique Ionic Liquids. *J. Chem. Theory Comput.* **2009**, *5*, 1038–1050.

(4) Plimpton, S. Fast Parallel Algorithms for Short-Range Molecular Dynamics. *J. Comp. Phys.* **1995**, *117*, 1–19.

(5) Horn, H. W.; Swope, W. C.; Pitera, J. W.; Madura, J. D.; Dick, T. J.; Hura, G. L.; Head-Gordon, T. Development of an improved four-site water model for biomolecular simulations: TIP4P-Ew. *J. Chem. Phys.* **2004**, *120*, 9665–9678.

(6) Tokuda, H.; Hayamizu, K.; Ishii, K.; Susan, M. A. B. H.; Watanabe, M. Physicochemical Properties and Structures of Room Temperature Ionic Liquids. 1. Variation of Anionic Species. *J. Phys. Chem. B* **2004**, *108*, 16593–16600.

(7) Del Pópolo, M. G.; Voth, G. A. On the Structure and Dynamics of Ionic Liquids. *J. Phys. Chem. B* **2004**, *108*, 1744–1752.

(8) Perkins, S. L.; Painter, P.; Colina, C. M. Molecular Dynamic Simulations and Vibrational Analysis of an Ionic Liquid Analogue. *J. Phys. Chem. B* **2013**, *117*, 10250–10260.